Inorganic Chemistry

Article

pubs.acs.org/IC

Controlling the Dipole−Dipole Interactions between Terbium(III) Phthalocyaninato Triple-Decker Moieties through Spatial Control Using a Fused Phthalocyaninato Ligand

Takaumi Morita,[†] Keiichi Katoh,*[,†,‡] Brian K. Breedlove,[†] and Masahiro Yamashita*[,†,‡]

[†]Department of Chemistry, Graduate School of Science, Tohoku University, 6-3 Aramaki-Aza-Aoba, Aoba-ku, Sendai, Miyagi 980-8578, Japan

[‡]CREST, JST, 4-1-8 Honcho, Kawaguchi, Saitama 332-0012, Japan

Supporting Information

ABSTRACT: Using a fused phthalocyaninato ligand to control the spatial arrangement of Tb^{III} moieties in Tb^{III} single-molecule magnets (SMMs), we could control the dipole−dipole interactions in the molecules and prepared the first tetranuclear Tb^{III} SMM complex. $[Tb(obPc)_2]Tb(Fused\text{-}Pc)Tb[Tb(obPc)_2]$ (abbreviated as $[\mathbf{Tb_4}]$; obPc = 2,3,9,10,16,17,23,24-octabutoxyphthalocyaninato, Fused-Pc = bis{7^2,8^2,12^2,13^2,17^2,18^2-hexabutoxytribenzo[*g*,*l*,*q*]-5,10,15,20-tetraazaporphirino}[*b*,*e*]benzenato). In direct-current magnetic susceptibility measurements, ferromagnetic interactions among the four Tb^{3+} ions were observed. In $[\mathbf{Tb_4}]$, there are two kinds of magnetic dipole−dipole interactions. One is strong interactions in the triple-decker moieties, which dominate the magnetic relaxations, and the other is the weak one through the fused phthalocyaninato (Pc) ligand linking the two triple-decker complexes. In other words, $[\mathbf{Tb_4}]$ can be described as a weakly ferromagnetically coupled dimer of triple-decker $Tb_2(obPc)_3$ complexes with strong dipole−dipole interactions in the triple-decker moieties and weak ones through the fused phthalocyaninato ligand linking the two triple-decker complexes. For $[\mathbf{Tb_4}]$, dual magnetic relaxation processes were observed similar to other dinuclear $Tb^{III}Pc$ complexes. The relaxation processes are due to the anisotropic centers. This is clear evidence that the magnetic relaxation mechanism depends heavily on the dipole−dipole (f−f) interactions between the Tb^{3+} ions in the systems. Through a better understanding of the magnetic dipole−dipole interactions obtained in these studies, we have developed a new strategy for preparing Tb^{III} SMMs. Our work shows that the SMM properties can be fine-tuned by introducing weak intermolecular magnetic interactions in a controlled SMM spatial arrangement.

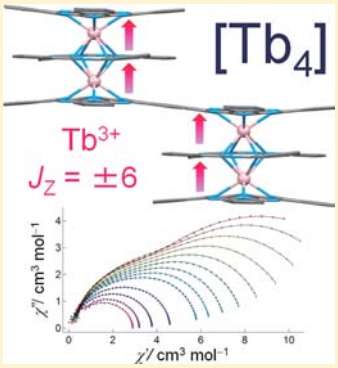

INTRODUCTION

The double-decker terbium(III) phthalocyaninato ($Tb^{III}Pc$) stacked complex (TBA)[$TbPc_2$] (TBA = tetrabutylammonium)[1] was shown to be a single-molecule magnet (SMM).[2] SMMs have several distinctive features, including slow magnetic relaxation and quantum tunneling of the magnetization (QTM),[3] which can be utilized for spintronic devices,[4] such as ultrahigh-density memory devices, quantum computers and so on. In order to use SMMs in these devices, it is necessary to elucidate their magnetic relaxation processes in detail.

In multiple-decker Pc dinuclear lanthanoid(III) SMMs, magnetic dipole−dipole interactions dominate the magnetic properties.[1,5] Triple-, quadruple-, and quintuple-decker complexes, which have two Tb^{III} ions, have been synthesized, and their magnetic relaxation processes have been investigated.[5c,e] We can control the intramolecular Tb−Tb distance by inserting diamagnetic Cd^{II} ions along the magnetic easy axis. Thus, the doubly degenerate ground state with magnetic dipole−dipole interactions between two Tb^{III} ions can be expressed as $J_z = \pm 12$ ($J_z = |\pm 6\rangle^a|\pm 6\rangle^b$) and $J_z = 0$ ($J_z = |\pm 6\rangle^a|\mp 6\rangle^b$).[5d,6] In addition, these complexes show dual magnetic relaxation processes in the low-temperature region because of the magnetic dipole−dipole interactions. Recently, dual relaxation processes have been observed for SMMs regardless of the type and number of metal ions present.[2b,5e,7] It is well-known that the magnetic relaxation properties reflect the local molecular symmetry and are extremely sensitive to tiny distortions in the coordination geometry. For example, tetranuclear Dy SMMs (Kramers system), in which four Dy^{III} ions are aggregated in a line, show a high anisotropic barrier of 173 K.[2b,7] However, in the case of the Tb^{III} ions (non-Kramers system), the ground state is only a bistate when the ligand field has axial symmetry. Therefore, the SMM properties of the tetranuclear Tb^{III} system have not been reported. In the cases when Pc ligands with axial symmetry have been used, tetranuclear terbium(III) phthalocyaninato complexes have not been obtained because the product is unstable because of a mismatch between the charge of the Pc ligands (2−) and the Tb^{III} ions.

In this article, we report the synthesis of a tetranuclear Tb^{III} SMM having magnetic dipole−dipole interactions between the four Tb^{3+} ions using a fused Pc derivative, which has two

Received: August 8, 2013
Published: November 13, 2013

   dx.doi.org/10.1021/ic4020459 | *Inorg. Chem.* 2013, 52, 13555−13561

Scheme 1. Synthesis of [Tb_4][a]

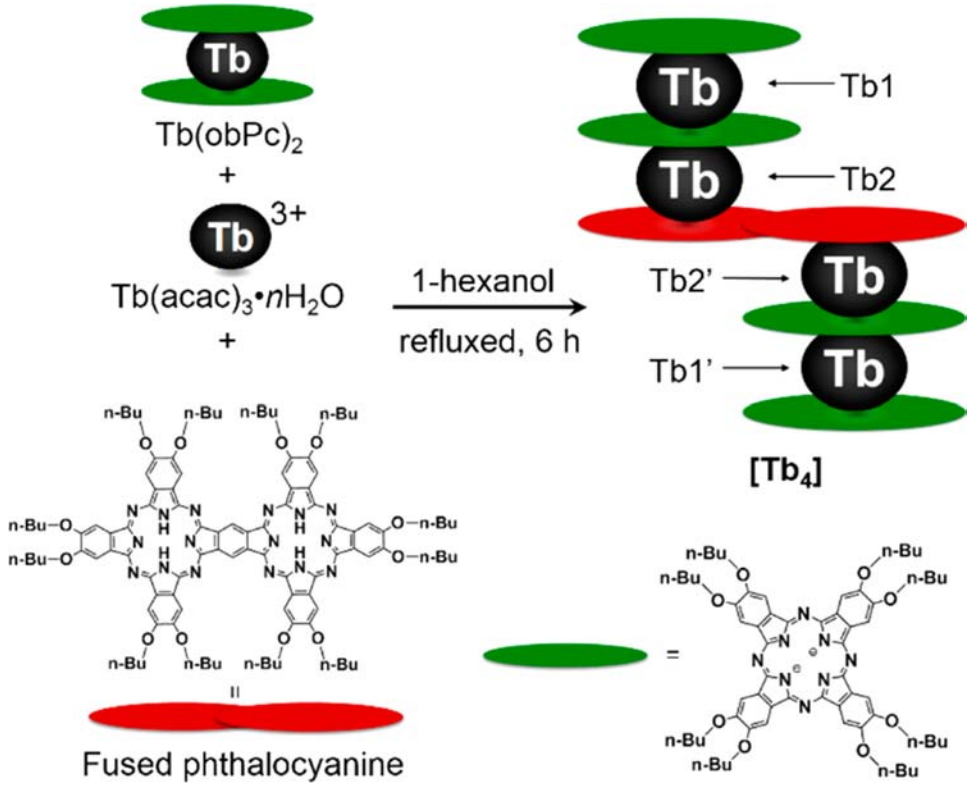

[a]There are two different coordination environments around the Tb^{III} ions. Tb1 is equal to Tb1′, and Tb2 is equal to Tb2′ on the basis of symmetry.

coordination sites. The fused Pc ligand, which was relatively easy to synthesize,[8] allowed us to control the overall charge of the complex. Finally, we will discuss the relationship between the magnetic properties and spatial arrangement of the Tb^{III} ions.

EXPERIMENTAL SECTION

All reagents were purchased from Wako, TCI, and Aldrich and used without further purification.

Preparation of Tb^{III} Double-Decker Tb(obPc)$_2$. Tb(obPc)$_2$ was synthesized by modifying a previously reported procedure.[9] 4,5-Dibutoxyphthalonitrile (650 mg, 2.38 mmol) and terbium(III) triacetate tetrahydrate (120 mg, 0.294 mmol) were refluxed in a mixture of *n*-hexanol (4 mL) and 1,8-diazabicyclo[5.4.0]undec-7-ene (40 μL). After 20 h of refluxing, the reaction mixture was chromatographed over silica gel (C-200 silica gel, Wako Pure Chemical Industries, Ltd.). The deep-green fraction was collected, and the solvent was evaporated to dryness. A dark-green powder was recrystallized from chloroform/ethanol (yield: 274 mg, 0.47 mmol, 19.7%).

Preparation of a Fused Phthalocyanine (Fused-Pc). A fused phthalocyanine (bis{7^2,8^2,12^2,13^2,17^2,18^2-hexabutoxytribenzo[*g*,*l*,*q*]-5,10,15,20-tetraazaporphirino}[*b*,*e*]benzene) was synthesized by modifying a previously reported procedure.[8b] 5,6-Dibutoxy-1,3-diiminoisoindoline (823 mg, 2.84 mmol), bis(1,3-diiminoisoindoline) (30 mg, 0.141 mmol), and magnesium diacetate dihydrate (203 mg, 0.947 mmol) were dried in vacuo at room temperature for 1 h. 2-(Dimethylamino)ethanol was added, and the solution was refluxed for 12 h. After refluxing, water (150 mL) was added, which caused the crude product to precipitate. The green precipitate was filtered and washed with methanol (50 mL) three times. The green solid was chromatographed over silica gel (C-200 silica gel, Wako Pure Chemical Industries, Ltd.). The collected deep-green fraction was concentrated and separated by column chromatography over BioBeads S-X1 with tetrahydrofuran (THF) as the eluent. The first fraction was collected, and the solvent was evaporated to dryness to obtain the fused phthalocyanine as a magnesium complex. To remove the magnesium, concentrated sulfuric acid (4 mL) was added, and the solution was stirred for 15 min. After 15 min, the crude product was diluted with water, and the insoluble material was collected by filtration and washed with water until the filtrate became neutral to obtain the metal-free fused phthalocyanine (yield: 35 mg, 1.9×10^{-2} mmol, 14%).

Preparation of [Tb(obPc)$_2$]Tb(Fused-Pc)Tb[Tb(obPc)$_2$] ([Tb_4]). Tb(acac)$_3$·*n*H$_2$O (100 mg) and Tb(obPc)$_2$ (200 mg, 8.6×10^{-2} mmol) were added to a refluxing *n*-hexanol suspension (4 mL) of bis{7^2,8^2,12^2,13^2,17^2,18^2-hexabutoxytribenzo[*g*,*l*,*q*]-5,10,15,20-tetraazaporphirino}[*b*,*e*]benzene[8b] (35 mg, 1.9×10^{-2} mmol). After 12 h of refluxing, methanol (100 mL) was added to the reaction mixture, which caused the crude product to precipitate. The crude product was separated using Celite and extracted with THF, and then the THF was evaporated to dryness to yield a blue solid. The solid was dissolved in THF, and the solution was chromatographed over silica gel (C-200 silica gel, Wako Pure Chemical Industries, Ltd.). The collected deep-blue solution was concentrated and separated by using column chromatography on BioBeads S-X1 with THF as the eluent. The first fraction was collected and evaporated to dryness. A dark-blue powder was obtained from chloroform/ethanol (yield: 3 mg, 4.4×10^{-4} mmol, 2.3%). ESI-MS: *m*/*z* 2268.37 (100%) [M^{3+}], 3403.06 (9.1%) [$(M + H)^{2+}$]. Elem anal. Calcd for $C_{362}H_{442}N_{48}O_{44}Tb_4$: C, 63.89; H, 6.55; N 9.88. Found: C, 64.02; H, 6.57; N, 9.82.

Preparation of the Magnetically Diluted Sample of [Tb_4]. Two samples diluted by Y_2(obPc)$_3$ (**1**) and THF (**2**) were prepared using the following procedures: **1** was prepared by dissolving [Tb_4] (5.05 mg) and Y_2(obPc)$_3$ (25.36 mg) in a molar ratio of 1:10[5d] in chloroform (5 mL). A suspension of the magnetically diluted sample was obtained by adding methanol. Solids were centrifuged and collected. Yield: 21.12 mg, which contained 3.5 mg of [Tb_4]. **2** was prepared by dissolving 5.35 mg of [Tb_4] in 0.5 mL of THF. This solution was injected into a gelatin capsule and cooled to 150 K. The sample weight was determined to be 2.5 mg by the $\chi_M T$ value of the direct-current (dc) magnetic measurement. The estimated molar ratio was 1:8000.

Physical Property Measurement. Elemental analysis and electrospray ionization mass spectroscopy (ESI-MS) were performed by the

dx.doi.org/10.1021/ic4020459 | *Inorg. Chem.* 2013, 52, 13555−13561

Research and Analytical Center for Giant Molecules, Tohoku University. IR spectra were measured as KBr pellets on a Jasco FT/IR-4200 spectrometer at 298 K. UV/vis/near-IR spectra in $CHCl_3$ were measured in a quartz cell with a path length of 1 cm on a Shimadzu UV-3100PC spectrometer at 298 K. Magnetic susceptibility measurements were performed on a Quantum Design superconducting quantum interference device (SQUID) magnetometer MPMS-XL. The dc measurements were collected in the T range of 2.0−300 K with a field strength of −7 to +7 T. Alternating-current (ac) measurements were performed at various frequencies in the range of 1−1500 Hz with an ac field amplitude of 3 Oe in a dc field (zero, 0.1, 0.2, 0.3, 0.35, 0.4, 0.45, 0.5, 0.6, 0.7, 0.8, 0.9, and 1.0 T). Measurements were performed on randomly oriented powder samples in a gelatin capsule. To prevent the sample from magnetically orienting, *n*-eicosane was used. A powdered sample of [**Tb$_4$**] suspended in *n*-eicosane was heated at 330 K for 1 min and cooled to 300 K. All data were corrected for the sample holder, *n*-eicosane, and diamagnetic contributions from the molecules using Pascal's constants.

RESULTS AND DISCUSSION

The fused Pc ligand was synthesized by modifying a previously reported procedure,[8b] and the tetranuclear $Tb^{III}Pc$ quintuple-decker complex [**Tb$_4$**] was prepared by refluxing a suspension of the fused phthalocyanine, $Tb(obPc)_2$ (obPc = 2,3,9,10,16,17,23,24-octabutoxyphthalocyaninato), and $Tb(acac)_3{\cdot}nH_2O$ in 1-hexanol for 12 h. The crude product was purified using column chromatography over silica gel and size-exclusion chromatography, followed by recrystallization from $CHCl_3$/EtOH, to obtain a dark-blue powder in 2.3% yield (Scheme 1). In lanthanoid-based SMMs, dipole−dipole interactions have the strongest effect on the magnetic properties, meaning that the distance between lanthanoid metals is extremely important. In [**Tb$_4$**], syn and anti isomers are possible, and their magnetic properties should be different. However, because of the bulky butoxy substituents on the Pc ligands, only the anti isomer was obtained. In [**Tb$_4$**], the distance between Tb1 and Tb2 was estimated to be 0.352 nm from $Tb_2(obPc)_3$, and the distance between Tb2 and Tb2′ was geometrically estimated to be 1.16 nm (Figure 1).

The dc magnetic susceptibility of [**Tb$_4$**] was measured in the temperature (T) range of 2.0−300 K using a SQUID magnetometer (Figure 2). The $\chi_M T$ value at room temperature

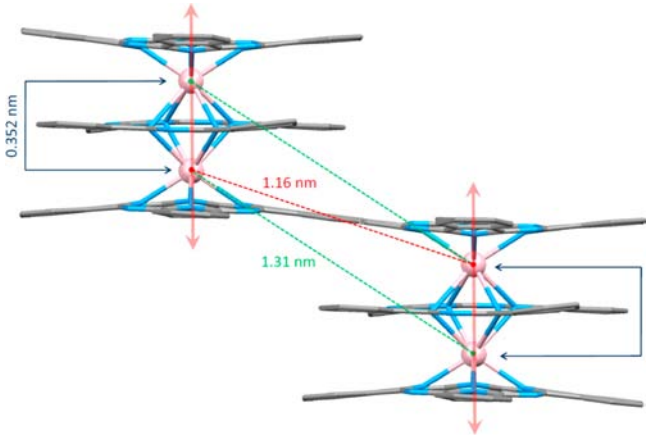

Figure 1. Simulated structure of [**Tb$_4$**] based on the reported triple-decker complex $Tb_2(obPc)_3$. This simulation was derived from the crystal structure of $Tb_2(obPc)_3$. The distance between Tb2 and Tb2′ was estimated geometrically to be 1.16 nm. Butoxy substituents are omitted for clarity.

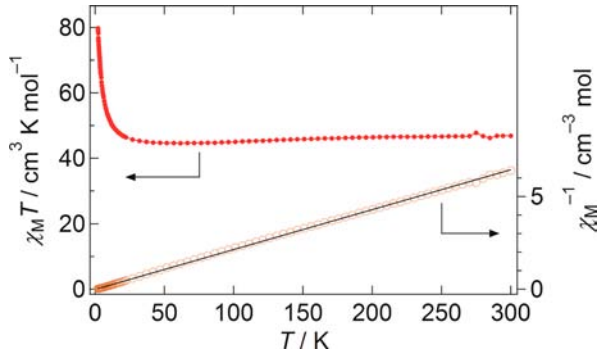

Figure 2. dc magnetic susceptibility of [**Tb$_4$**].

was 46.91 cm^3 K mol^{-1}, which is consistent with the expected value of 47.27 cm^3 K mol^{-1} for four free Tb^{3+} ions ($^7F_6$, $S = 3$, $L = 3$, and $g = {}^3/_2$). In addition, the magnetic susceptibility of [**Tb$_4$**] obeyed the Curie−Weiss law, giving a Curie constant (C) of 46.48 cm^3 K mol^{-1} and a positive Weiss constant (θ) of 0.07 K over the entire T range. A $\chi_M T$ versus T plot of the data for [**Tb$_4$**] increased with a decrease in T and reached a maximum of 79.77 cm^3 K mol^{-1} at 2.0 K, which indicated the existence of ferromagnetic interactions among the four Tb^{III} ions. Each [**Tb$_4$**] molecule is isolated because of the bulky butoxy substituents. This is supported by dc magnetic measurements on a sample diluted with diamagnetic $Y_2(obPc)_3$ (**1**) and THF (**2**), which show that intermolecular magnetic interactions are negligible (Figure S4 in the Supporting Information, SI). In lanthanoid(III) phthalocyaninato SMM systems, magnetic dipole−dipole interactions highly affect their magnetic properties. Hence, the magnetic dipoles (complexes) must be magnetically diluted in the dilution matrix in the proper ratio. In this case, the ratio of [**Tb$_4$**] and $Y_2(obPc)_3$ was 1:10 in **1** and that of [**Tb$_4$**] and THF was 1:8000 in **2**, which was a large enough ratio for complete dilution. Therefore, we can conclude that the ferromagnetic interactions in [**Tb$_4$**] are due to the intramolecular interactions only.

In addition, the anti conformation is important for ferromagnetic dipole−dipole interactions because of the relative angle of neighboring Tb^{III} ions. If the complex is in a syn arrangement, antiferromagnetic interactions will occur because of the nature of the magnetic dipole.[5e] We can estimate the ferromagnetic dipole−dipole interactions ($D_{ij} \propto 1/r_{ij}^3$, where r_{ij} is the distance between spins i and j) between each Tb^{III} ion. D_{ij} between Tb2 and Tb2′ is ca. ${}^1/_{38}$ that between Tb1 and Tb2 because the distance (r_{ij}) between Tb2 and Tb2′ (1.16 nm) is approximately 3 times longer than that between Tb1 and Tb2 (0.352 nm) (Figure 1).[5d]

Here, we estimated the strength of the interaction in Tb2−Tb2′ distances from the $\chi_M T$ value for $Tb_2(obPc)_3$. The Tb1−Tb2 and Tb1′−Tb2′ distances in [**Tb$_4$**] are almost the same as that in $Tb_2(obPc)_3$, which suggests that the magnetic dipole−dipole interactions have the same strength. Hence, the contribution to the $\chi_M T$ value from the interaction between Tb2 and Tb2′ can be evaluated from $\Delta\chi_M T = \chi_M T([\mathbf{Tb_4}]) - 2\chi_M T(Tb_2(obPc)_3)$ (Figure 3). In Figure 3, the $\Delta\chi_M T$ value increased in the low-T region because of ferromagnetic interactions between Tb2 and Tb2′. However, the value of $\Delta\chi_M T$ (i.e., the coupling strength of Tb2−Tb2′) was much lower than the $\chi_M T$ value of [**Tb$_4$**]. Consequently, the ferromagnetic interaction between Tb2 and Tb2′ is weak.

dx.doi.org/10.1021/ic4020459 | *Inorg. Chem.* 2013, 52, 13555−13561

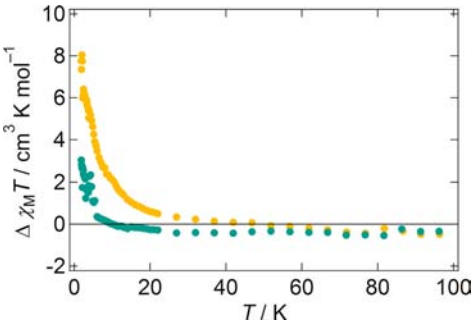

Figure 3. Evaluation of the coupling strength between Tb2 and Tb2′ from the dc magnetic measurement. $\Delta\chi_M T$ was calculated from the following formula: $\Delta\chi_M T = \chi_M T([\mathbf{Tb_4}]) - 2\chi_M T(Tb_2(obPc)_3)$ for orange dots and $\Delta\chi_M T = \chi_M T(\mathbf{1}) - 2\chi_M T(Tb_2(obPc)_3)$ for green dots.

In contrast, the magnetic interactions in Tb1−Tb2 and Tb1′−Tb2′ were much stronger than that of Tb2−Tb2′, meaning that the magnetic properties of [$\mathbf{Tb_4}$] resemble those of the triple-decker complex. In other words, [$\mathbf{Tb_4}$] can be described as a weakly ferromagnetically coupled dimer of triple-decker complexes. From one viewpoint, each half of the Tb^{III} dimer in [$\mathbf{Tb_4}$] acts as a field bias on its neighbor, shifting the tunnel resonances to new positions relative to the magnitude of the magnetic dipole−dipole interactions between the Tb^{III} ions. Considering only the f−f interaction between the Tb^{III} ions, the magnetic interactions in Tb1−Tb2 and Tb1′−Tb2′ are on the different order of field bias. Therefore, using this complex, we can investigate the interactions between triple-decker complexes, which show SMM behaviors. The $M-H$ curve at 1.8 K for [$\mathbf{Tb_4}$] showed no magnetic hysteresis similar to that for $Tb_2(obPc)_3$, meaning that the spins were not frozen under these conditions (Figure S5 in the SI).[1,5d]

In ac magnetic susceptibility measurements on a powder sample of [$\mathbf{Tb_4}$], shown in Figure 4, sharp drops in the in-phase (χ_M') and out-of-phase (χ_M'') peaks in different T ranges dependent on the frequency (f) were observed, indicating that [$\mathbf{Tb_4}$] was an SMM. The barrier height for reversal of the magnetic moment (Δ/hc) was estimated to be 149 cm^{-1} with a frequency factor (τ_0) of 2.7×10^{-8} s from an Arrhenius plot using $\tau = \tau_0 \exp(\Delta/k_BT)$ and $\tau = 1/(2\pi f)$, where τ is the magnetic relaxation time and Δ is the energy barrier (Figure 5). This linear relationship between $\ln(\tau)$ and T^{-1} indicates that an Orbach process is dominant in the higher-T range (the Orbach process is due to spin−lattice interactions[10]) and independent of the dc magnetic field (H_{dc} = 0.1−0.4 T). The triple-decker complex $Tb_2(obPc)_3$ has a Δ/hc value of 230 cm^{-1}, which is on the same order of magnitude as that for [$\mathbf{Tb_4}$].[5e] In a $\chi_M''T$ versus T plot in a zero field and an ac field of 1488 Hz, only a single peak at 25 K was observed (Figure 4). The dinuclear Tb^{III} complex [(Pc)Tb(Pc)Tb(obPc)] with different coordination environments reported by Ishikawa et al. exhibits two clear $\chi_M''T$ peaks at 20 and 27 K.[6] In other words, our results indicated that the four Tb^{III} ions in [$\mathbf{Tb_4}$] are in similar coordination environments.

From the simulated structure, Tb1 and Tb2 seemed to be in different environments because interactions between Tb2 and Tb2′ were observed in the dc magnetic susceptibility measurements. However, the ac magnetic susceptibility shows that the four Tb^{3+} ions in [$\mathbf{Tb_4}$] are equivalent, meaning that we only need to consider the magnetic dipole−dipole interactions. In Figures S7−S10 in the SI, the ac magnetic susceptibilities of **1** and **2** are given, which have behavior quite similar to those of the

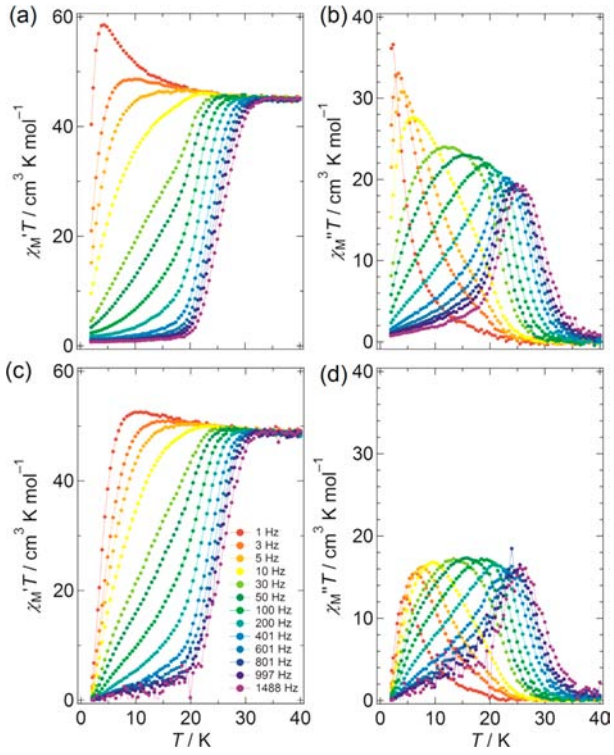

Figure 4. Frequency (f) and temperature (T) dependencies of (a and c) the real and (b and d) imaginary parts of the ac magnetic susceptibility. Parts a and b were measured in the absence of a magnetic field, and parts c and d were done in the presence of a magnetic field of 0.4 T. In all graphs, the solid lines are guides for the eyes.

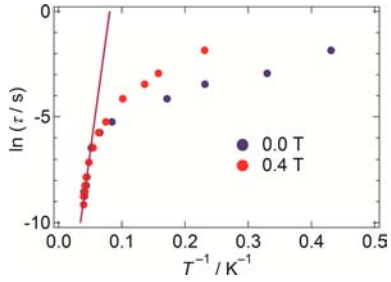

Figure 5. Arrhenius plot made using the data from Figure 4. The straight lines are least-squares fits of the data, which yielded the following parameters: Δ/hc = 149 cm^{-1}, $\tau_0 = 2.7 \times 10^{-8}$ s at 0 T and Δ/hc = 151 cm^{-1}, $\tau_0 = 2.7 \times 10^{-7}$ s at 0.4 T.

pure [$\mathbf{Tb_4}$] complex. These data also support that [$\mathbf{Tb_4}$] is an SMM.

Figures 6 and 7 show plots of the f dependence of the magnetization performed to elucidate the details of the magnetic relaxation dynamics. Argand plots (i.e., χ_M' versus χ_M'' plots) in the T range of 4−23 K and f range of 1−1500 Hz in a dc field of 0 T showed clear semicircular shapes, which could be fitted using a generalized Debye model (eq 1), indicating that a single relaxation process occurred (Figures 6 and S6 in the SI).[11]

$$\chi(\omega) = \chi_s + \frac{\chi_T - \chi_S}{1 + (i\omega\tau)^{1-\alpha}} \quad (1)$$

In the entire T range measured, the α parameter, which quantifies the width of the τ distribution, was in the range of 0.19−0.26 at 0 T and was temperature-dependent. This behavior

dx.doi.org/10.1021/ic4020459 | Inorg. Chem. 2013, 52, 13555−13561

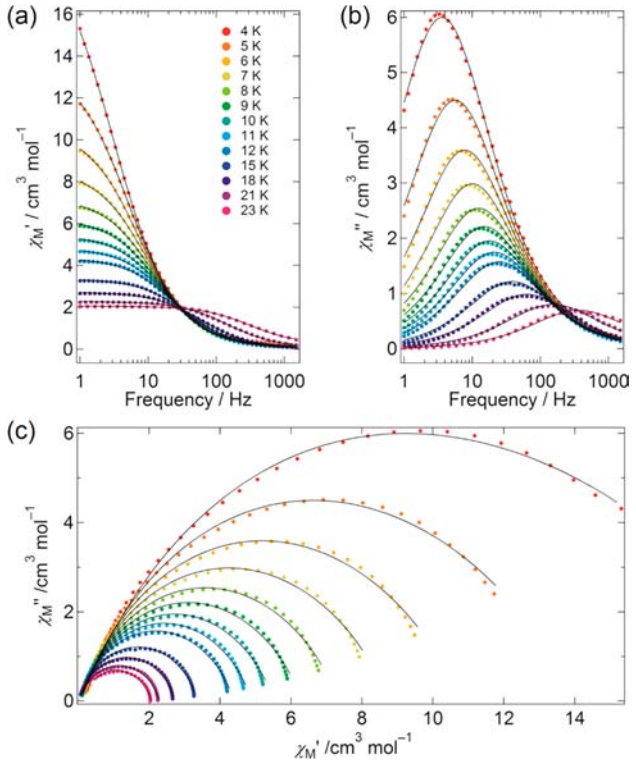

Figure 6. (a) χ_M' and (b) χ_M'' versus f plots in a dc field of 0 T and (c) an Argand plot for [**Tb$_4$**]. Black solid lines were fitted using a generalized Debye model (see eqs 1−3 in the SI). This plot showed clear semicircular shapes, indicating that a single relaxation process occurred.

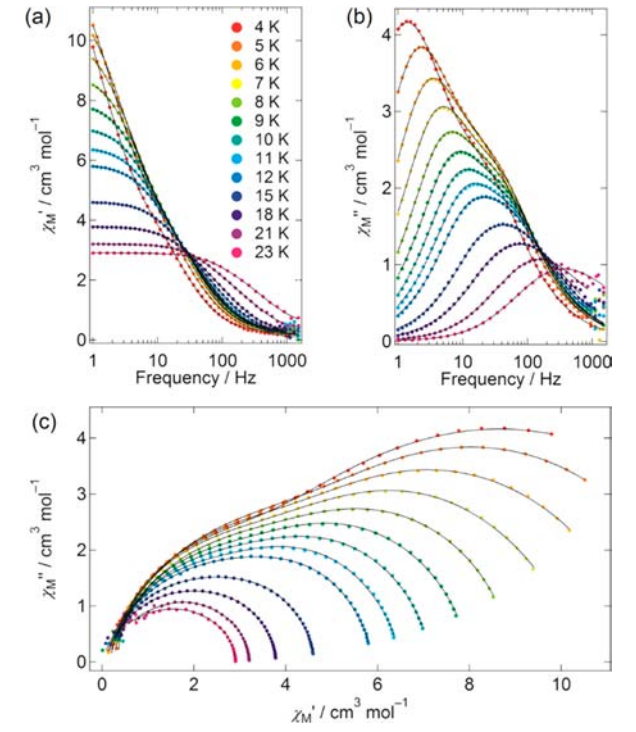

Figure 7. (a) χ_M' and (b) χ_M'' versus f plots in a dc field of 0.4 T and (c) an Argand plot for [**Tb$_4$**]. Black solid lines were fitted using generalized and extended Debye models (eqs 4−6 in the SI).

has already been reported for dinuclear Tb^{III}Pc multiple-decker complexes.[5e]

In Argand plots for the measurements in a dc field of 0.4 T (Figure 7c), the magnetic relaxation process splits into dual processes (τ_1, high-f part; τ_2, low-f part) with a decrease in T in the range of 4−15 K. In order to understand the different relaxation mechanisms corresponding to the two observed peaks, an extended Debye model, which is a linear combination of the generalized Debye model, was used to fit τ_1 and τ_2[12] (eq 2).

$$\chi(\omega) = \chi_s + \frac{\chi_T - \chi_S}{1 + (i\omega\tau_1)^{1-\alpha_1}} + \frac{\chi_T - \chi_S}{1 + (i\omega\tau_2)^{1-\alpha_2}} \quad (2)$$

There are clear differences between the high- and low-T regions (Figure 9a). Above 15 K, an Orbach process is dominant. Below 15 K, the curve gradually splits into a T-independent regime for τ_1 and a T-dependent regime for τ_2. The behavior of τ_1 is consistent with the appearance of quantum effects acting on QTM.[1−4,5c−e]

On the other hand, if τ_2 involves a Raman process,[7,13] the data should conform to $1/\tau \propto T^7$ (non-Kramers system).[5e,14] However, the phenomenon does not follow the above relationship, meaning that it is not dominated by a Raman process.[13d] Thus, we concluded that a crossover from a thermally activate Orbach process was dominant in the high-T region and a direct or phonon-induced tunneling process occurred below 15 K.[5e,7]

An Argand plot in several H_{dc} at 5 K is shown in Figure 8. The magnetic relaxation changes from a single process to a dual one

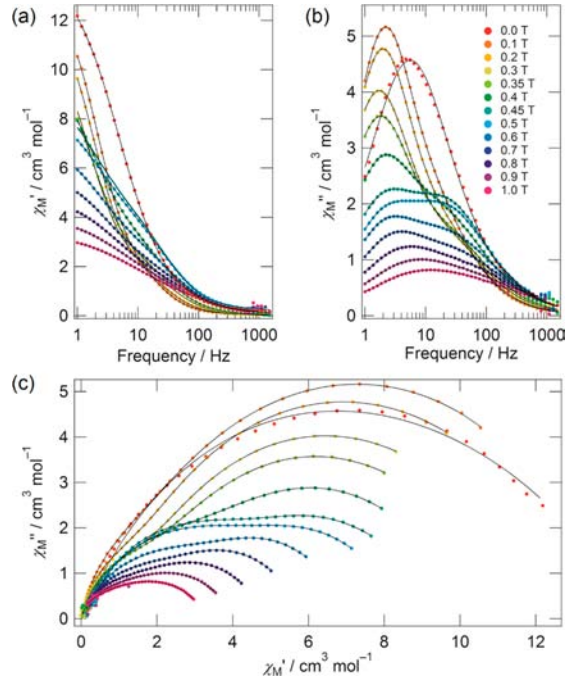

Figure 8. (a) χ_M' and (b) χ_M'' versus f plots at 5 K and (c) an Argand plot for [**Tb$_4$**]. Black solid lines were fitted using generalized and extended Debye models. In a dc field of 0.0 T, the lines have semicircular shapes, indicating that a single relaxation process occurred. The other lines were not semicircular, indicating the presence of dual relaxation processes.

with an increase in H_{dc} in the range of 0−1.0 T. In the case of the Argand plots in a field of 0.1 T, the magnetic relaxations of [**Tb$_4$**] showed dual relaxation processes (Figure 9b). For diluted sample **1**, behavior similar to that of [**Tb$_4$**] was observed, as shown in Figures S14 and S15 in the SI.

dx.doi.org/10.1021/ic4020459 | Inorg. Chem. 2013, 52, 13555−13561

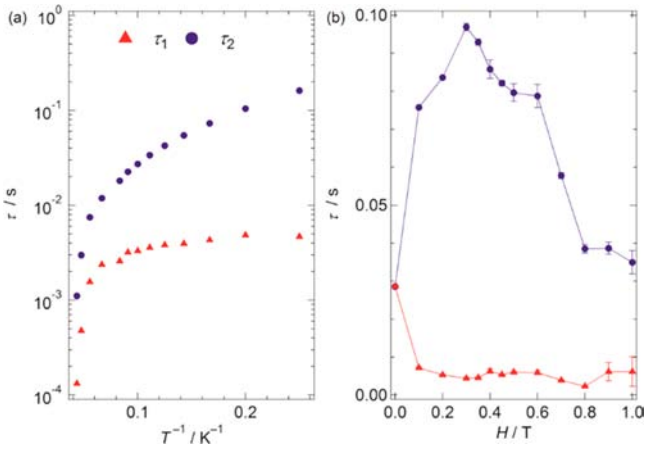

Figure 9. (a) Arrhenius plots made by using parameters obtained from the Argand plots (Figure 7) for [**Tb**$_4$] in a dc magnetic field of 0.4 T. The temperature-independent part (τ_1) of the high-f relaxation process involves QTM. (b) Relaxation time (τ) versus magnetic field plot for [**Tb**$_4$] made by using parameters obtained from the Argand plots (Figure 8).

Previously, we have suggested that two conditions must be met for dual magnetic relaxation processes to occur in dinuclear Tb^{III}Pc SMMs.[5d,e] (1) Two Tb^{III} ions must be crystallographically equivalent or nearly equivalent in the molecule. In the case of [**Tb**$_4$], a $\chi_M''T$ versus T plot showed only a single peak, indicating that the Tb^{III} sites are nearly equivalent. (2) The spatial arrangement and distance between the Tb^{III} ions in the molecule must bring about ferromagnetic dipole−dipole coupling. This agrees with the dc magnetic susceptibility measurements on [**Tb**$_4$]. As stated above, [**Tb**$_4$] meets these conditions.

In addition, the ac magnetic properties of [**Tb**$_4$] are similar to those reported for the triple-decker complex $Tb_2(obPc)_3$,[5d] especially the magnetic field dependence of τ (Figure 9). The order of magnitude of τ_1 was 10^{-3}, and that of τ_2 was 10^{-2}, which are the same as those reported for $Tb_2(obPc)_3$. We believe that, in the $Tb_2(obPc)_3$ unit in [**Tb**$_4$], the internal magnetic field is very strong and dominates the magnetic properties of [**Tb**$_4$]. In contrast, the $Tb_2(obPc)_3$ unit in [**Tb**$_4$] feels a much smaller internal magnetic field from the neighboring one because of the long distance. Thus, [**Tb**$_4$] is described as a weakly ferromagnetically coupled dimer of $Tb_2(obPc)_3$ units. As a result, we think that, if the two Tb^{3+} ions are isolated by more than 1.2 nm, the magnetic dipole−dipole interactions, which affect the spin dynamics, can be ignored.

In the spatially closed double-decker $Tb(obPc)_2$ dimer system ($\varphi = 45°$: rotation angle of stacking Pc rings), polycrystalline and diluted samples showed totally different magnetic behavior.[5e,12] Dual relaxation processes were observed for the polycrystalline sample, whereas the diluted sample showed a single relaxation process. On the other hand, $Tb_2(obPc)_3$ ($\varphi = 32°$) and [**Tb**$_4$], polycrystalline and diluted samples, showed qualitatively the same magnetic behavior.[5d] Thus, for dual magnetic relaxation processes to occur in Tb^{III}Pc SMMs, intramolecular dipole−dipole interactions between Tb^{III} ions are more important than the coordination geometry is. In addition, intermolecular interactions often strongly affect their magnetic properties. The results clearly show that, if we control the dipole−dipole interactions by controlling the spatial arrangement of the Tb^{III}Pc SMMs, the interactions between them can be elucidated.

CONCLUSION

In conclusion, a new tetranuclear Tb^{III}Pc quintuple-decker SMM, [**Tb**$_4$], with a fused Pc ligand and ferromagnetic interactions between four Tb^{III} ions was synthesized. The ferromagnetic interactions between the triple-decker moieties (Tb1−Tb2 and Tb1′−Tb2′) were found to pass through the Tb2 and Tb2′ sites, causing the magnetic properties to be similar to those of $Tb_2(obPc)_3$. Our results suggest that the dual magnetic relaxation properties of Tb^{III}Pc multiple-decker systems has a magic number of $2n$, where n is the number of triple-decker units (n = 1 and 2), i.e., the number of Tb^{III} sites. We believe that an even number of Tb^{III} ions in multiple-decker Pc complexes causes the dual magnetic relaxation processes in the low-T region. Although there are f−f interactions between Tb2 and Tb2′, they are weak because the Tb2−Tb2′ distance is long, meaning that magnetic properties are barely affected.

As stated above, magnetic dipole−dipole interactions dominate the magnetic behaviors of lanthanoid(III) phthalocyaninato SMMs. Therefore, more detailed investigations on the relationship between the magnetic properties, such as dual magnetic relaxation processes, and the spatial arrangement of SMMs are needed. Currently, we are synthesizing multinuclear complexes with different multicoordinating Pc ligands, which have different spatial arrangements of the Tb^{III} ions (f−f interactions), in order to control the magnetic dipole−dipole interactions.

ASSOCIATED CONTENT

Supporting Information

Additional experimental data for [**Tb**$_4$] and the diluted sample of [**Tb**$_4$]. This material is available free of charge via the Internet at http://pubs.acs.org.

AUTHOR INFORMATION

Corresponding Authors

*Phone: +81-22-795-3878. Fax: +81-795-6548. E-mail: kkatoh@m.tohoku.ac.jp.

*Phone: +81-22-795-6544. Fax: +81-795-6548. E-mail: yamasita@agnus.chem.tohoku.ac.jp.

Author Contributions

The authors contributed equally.

Notes

The authors declare no competing financial interest.

ACKNOWLEDGMENTS

This work was financially supported by Research Fellowships of Japan Society for the Promotion of Science for Young Scientists, Tohoku University Institute for International Advanced Research and Education Organization (IAREO), a Grant-in-Aid for Scientific Research (S) (Grant 20225003), and a Grant-in-Aid for Young Scientists (B) (Grant 24750119) from the Ministry of Education, Culture, Sports, Science, and Technology, Japan.

REFERENCES

(1) Ishikawa, N.; Sugita, M.; Ishikawa, T.; Koshihara, S.; Kaizu, Y. *J. Am. Chem. Soc.* **2003**, *125*, 8694−8695.

(2) (a) Sessoli, R.; Gatteschi, D.; Caneschi, A.; Novak, M. A. *Nature* **1993**, *365*, 141−143. (b) Woodruff, D. N.; Winpenny, R. E.; Layfield, R. A. *Chem. Rev.* **2013**, *113*, 5110−5148.

(3) (a) Thomas, L.; Lionti, F.; Ballou, R.; Dante, G.; Roberta, S.; Barbara, B. *Nature* **1996**, *383*, 145−147. (b) Gatteschi, D.; Sessoli, R.;

Villain, J. *Molecular Nanomagnets*; Oxford University Press: New York, 2007. (c) Ishikawa, N.; Sugita, M.; Wernsdorfer, W. *Angew. Chem., Int. Ed.* **2005**, *44*, 2931−2935. (d) Ishikawa, N.; Sugita, M.; Wernsdofer, W. *J. Am. Chem. Soc.* **2005**, *127*, 3650−3651.
(4) (a) Katoh, K.; Yoshida, Y.; Yamashita, M.; Miyasaka, H.; Breedlove, B. K.; Kajiwara, T.; Ishikawa, N.; Isshiki, H.; Zhang, Y. F.; Komeda, T.; Yamagishi, M.; Takeya, J. *J. Am. Chem. Soc.* **2009**, *131*, 9967−9976. (b) Urdampilleta, M.; Klyatskaya, S.; Cleuziou, J. P.; Ruben, M.; Wernsdorfer, W. *Nat. Mater.* **2011**, *10*, 502−506. (c) Komeda, T.; Isshiki, H.; Liu, J.; Zhang, Y. F.; Lorente, N.; Katoh, K.; Breedlove, B. K.; Yamashita, M. *Nat. Commun.* **2011**, *2*, 217:1−7.
(5) (a) Ishikawa, N.; Iino, T.; Kaizu, Y. *J. Am. Chem. Soc.* **2002**, *124*, 11440−11447. (b) Wang, H.; Liu, T.; Wang, K.; Duan, C.; Jiang, J. *Chemistry* **2012**, *18*, 7691−7694. (c) Fukuda, T.; Kuroda, W.; Ishikawa, N. *Chem. Commun.* **2011**, *47*, 11686−11688. (d) Katoh, K.; Kajiwara, T.; Nakano, M.; Nakazawa, Y.; Wernsdorfer, W.; Ishikawa, N.; Breedlove, B. K.; Yamashita, M. *Chem.—Eur. J.* **2011**, *17*, 117−122. (e) Katoh, K.; Horii, Y.; Yasuda, N.; Wernsdorfer, W.; Toriumi, K.; Breedlove, B. K.; Yamashita, M. *Dalton Trans.* **2012**, *41*, 13582−13600.
(6) Ishikawa, N.; Otsuka, S.; Kaizu, Y. *Angew. Chem., Int. Ed.* **2005**, *44*, 731−733.
(7) Guo, Y.-N.; Xu, G.-F.; Gamez, P.; Zhao, L.; Lin, S.-Y.; Deng, R.; Tang, J.; Zhang, H.-J. *J. Am. Chem. Soc.* **2010**, *132*, 8538−8539.
(8) (a) Gryko, D.; Li, J.; Diers, J. R.; Roth, K. M.; Bocian, D. F.; Kuhr, W. G.; Lindsey, J. S. *J. Mater. Chem.* **2001**, *11*, 1162−1180. (b) Tolbin, A. Y.; Pushkarev, V. E.; Tomilove, L. G.; Zefirov, N. S. *Russ. Chem. Bull., Int. Ed.* **2006**, *55*, 1155−1158.
(9) Katoh, K.; Yamamoto, K.; Kajiwara, T.; Takeya, J.; Breedlove, B. K.; Yamashita, M. *J. Phys.: Conf. Ser.* **2011**, *303*, 012035:1−10.
(10) (a) Orbach, R. *Proc. Phys. Soc.* **1961**, *A77*, 821−826. (b) Finn, C. B. P.; Orbach, R.; Wolf, W. P. *Proc. Phys. Soc.* **1961**, *A77*, 261−268.
(11) Cole, K. S.; Cole, R. H. *J. Chem. Phys.* **1941**, *9*, 341−351.
(12) Domingo, N.; Luis, F.; Nakano, M.; Muntó, M.; Gómez, J.; Chaboy, J.; Ventosa, N.; Campo, J.; Veciana, J.; Ruiz-Molina, D. *Phys, Rev. B* **2009**, *79*, 214404:1−9.
(13) (a) Waller, I. *Z. Phys.* **1932**, *79*, 370−388. (b) Van Vleck, J. H. *J. Chem. Phys.* **1939**, *7*, 72−84. (c) Van Vleck, J. H. *Phys. Rev.* **1940**, *57*, 426−447. (d) Kronig, R. d. L. *Physica* **1939**, *6*, 33−43.
(14) Abragam, A.; Bleaney, B. *Electron Paramagnetic Resonance of Transition Ions*; Oxford University Press: London, 1970.